Available online at www.sciencedirect.com
SCIENCE DIRECT
Journal of African Earth Sciences 43 (2005) 525–536
Journal of African Earth Sciences
www.elsevier.com/locate/jafrearsci

Petrological and mineralogical studies of Pan-African serpentinites at Bir Al-Edeid area, central Eastern Desert, Egypt

M.K. Azer *, A.E.S. Khalil

Geology Department, National Research Centre, Al-Behoos Street, Dokki, Cairo 12622, Egypt

Received 14 February 2005; received in revised form 3 July 2005; accepted 11 September 2005
Available online 28 November 2005

Abstract

The studied serpentinites occur as isolated masses, imbricate slices of variable thicknesses and as small blocks or lenses incorporated in the sedimentary matrix of the mélange. They are thrusted over the associated island arc calc-alkaline metavolcanics and replaced by talc-carbonates along shear zones. Lack of thermal effect of the serpentinites upon the enveloping country rocks, as well as their association with thrust faults indicates their tectonic emplacement as solid bodies. Petrographically, they are composed essentially of antigorite, chrysotile and lizardite with subordinate amounts of carbonates, chromite, magnetite, magnesite, talc, tremolite and chlorite. *Chrysotile* occurs as cross-fiber veinlets traversing the antigorite matrix, which indicate a late crystallization under static conditions. The predominance of antigorite over other serpentine minerals indicates that the serpentinites have undergone prograde metamorphism or the parent ultramafic rocks were serpentinized under higher pressure. The parent rocks of the studied serpentinites are mainly harzburgite and less commonly dunite and wehrlite due to the prevalence of mesh and bastite textures. The serpentinites have suffered regional metamorphism up to the greenschist facies, which occurred during the collisional stage or back-arc basin closure, followed by thrusting over a continental margin. The microprobe analyses of the serpentine minerals show wide variation in SiO_2, MgO, Al_2O_3, FeO and Cr_2O_3 due to different generations of serpentinization. The clinopyroxene relicts, from the partly serpentinized peridotite, are augite and similar to clinopyroxene in mantle-derived peridotites. The chromitite lenses associated with the serpentinites show common textures and structures typical of magmatic crystallization and podiform chromitites. The present data suggest that the serpentinites and associated chromitite lenses represent an ophiolitic mantle sequence from a supra-subduction zone, which were thrust over the continental margins during the collisional stage of back-arc basin.

Keywords: Pan-African serpentinites; Chromite; Clinopyroxene; Supra-subduction zone

1. Introduction

Serpentinites are composed almost exclusively of minerals of the serpentine group, formed through hydrothermal alteration of previously existing minerals of ultramafic rocks, such as olivine and pyroxene. They are produced when hot seawater circulates through the lithosphere at spreading ocean ridges or in regions where mountain-building activities have been occurred in response to the closing of an ocean basin.

Ophiolitic ultramafic rocks are very common in the Eastern Desert of Egypt as part of the Pan-African belt and are represented by serpentinites enclosing rare peridotite relics. A dismembered ophiolite succession was first recorded at Wadi Ghadir, central Eastern Desert (El Sharkawy and El Bayoumi, 1979); since then, the serpentinites of Egypt were interpreted as an ocean floor ophiolite suite tectonically obducted in convergent zones (Shackleton et al., 1980; Ries et al., 1983; El Gaby et al., 1984, 1988; Abu El Ela, 1996; and others). Akaad (1996, 1997) and Akaad and Abu El Ela (2002) classified the serpentinites in the Eastern Desert according to their mode of occurrence into: (1) Allochtonous serpentinites including

* Corresponding author. Tel.: +20 2 7742962; fax: +20 2 3370931.
E-mail address: mokhles72@yahoo.com (M.K. Azer).

1464-343X/$ - see front matter © 2005 Elsevier Ltd. All rights reserved.
doi:10.1016/j.jafrearsci.2005.09.008

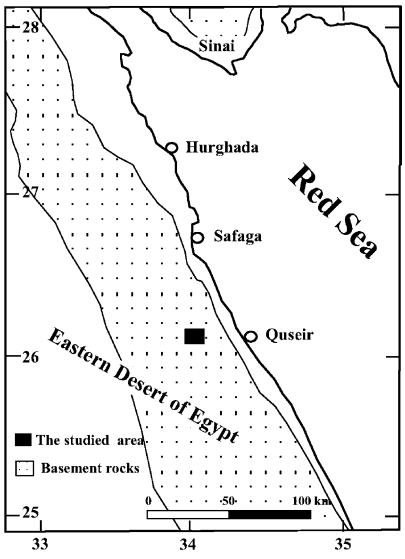

Fig. 1. Location map of the studied area.

boulders in the Hafafit-type gneisses and boulders in the arc volcaniclastic mélanges, and (2) flow-intruded serpentinites. The former is appearing as allochtonous bodies within arc assemblages, while the latter was intruded their host rocks. As regards other previous works; Ahmed (1983, 2005) considered the serpentinites in the Eastern Desert as nonophiolitic intrusive hot ultramafic magma, as they have notable thermal effect of high grade on the adjoining submarine lava flow sheets.

Detailed geological, petrographical and geochemical studies on the serpentinite rocks at Bir Al-Edeid area (Fig. 1) are lacking. The occurrence was mentioned briefly and mapped by El Ramly (1972), Shazly and Heikal (1980), Akaad and Abu El Ela (2002), Asran and Kabesh (2003), and El Bahariya and Arai (2003). The aim of the present contribution is to study the geology, petrology, mineral chemistry and geochemistry of the serpentinites in Bir Al-Edeid area, in older to elucidate their origin and tectonic setting.

2. Analytical techniques

Chemical compositions of the essential rock-forming minerals in the studied serpentinites were determined using a CAMECA SV 50 electron microprobe under operating conditions of 15 kV and 15 nA. Suitable synthetic and natural mineral standards were applied for calibration. The chemical analyses of the different representative mineral crystals were carried out at Würzburg University, Germany. Major and trace elements were determined for 15 samples of the massive serpentinites and for two chromitite samples by the X-ray fluorescence spectrometry (Philips Pw 2400) at the Institute of Geology and Mineralogy, Friederich–Alexander University, Erlangen–Nûrenberg, Germany. Concentrations of the major oxides were obtained on fused lithium-tetraborate discs, while the trace elements were determined on pressed pellets. Ferrous iron was determined by titration with standard $KMnO_4$. The amount of iron in the ferrous state (FeO) was subtracted from the total iron to obtain the ferric iron (Fe_2O_3) content. Losses on ignition (LOI) were determined by heating powdered samples for 50 min at 1000 °C.

3. Geologic setting and field observations

The area under investigation lies between latitudes 26°07′05″ and 26°11′50″N, and longitudes 33°50′00″ and 33°57′27″E (Fig. 2). It is occupied by Meatiq gneisses, schists, ophiolitic rocks, calc-alkaline metavolcanics and associated metapyroclastics in addition to older granites and Dokhan Volcanics. The Meatiq gneisses are composed of variably deformed and cataclastic gneisses, amphibolites and gneissose granite (El Gaby, 1984; Habib et al., 1985; Habib, 1987). The schists were described by Akaad and Noweir (1972, 1980) as Abu Fannani Formation, which comprise a distinctly interbedded succession of pelitic, semipelitic and calcareous pelitic schists together with subordinate mature metaquartzites and immature metagreywakes. Ophiolitic rocks consist of serpentinite and metagabbroic rocks. The ophiolitic rocks overlie calc-alkaline metavolcanics which consist of metaandesite, metadacite and metabasaltic rocks. The contact between the ophiolitic rocks and the metavolcanic rocks is interpreted to be a thrust fault (Asran and Kabesh, 2003). The Dokhan Volcanics exposed in the mapped area comprise andesites and dacites of calc-alkaline nature and subduction-related tectonic setting (Shazly and Heikal, 1980; Akaad and Abu El Ela, 2002; Asran et al., 2005).

Serpentinites, the subject of the present work, occur as isolated bodies and imbricated slices of variable thicknesses tectonically mixed with schists, calc-alkaline metavolcanics and mélange. They also occur as small lenses in the metasedimentary matrix of the mélange trending NW–SE and N–S conformable with the regional structure. These lenses are well exposed along both sides of Qift-Quseir asphaltic road and along Wadi El-Haramiya. The serpentinites are generally massive, but become sheared and foliated along the peripheries of the lenses. The foliation of the intensively sheared serpentinites is parallel to the schistosity of the surrounding metavolcanic rocks. Along shear zones, the serpentinite bodies are replaced by talc-carbonate rocks due to CO_2 metasomatism (Akaad and El Ramly, 1961; Basta and Abdel Kader, 1969; Basta and Hanafy, 1971; Akaad and Noweir, 1972). Fresh peridotite relics occur as minor bodies within the serpentinite masses, a feature not recorded in the studied area before. Also, thin pyroxenite dykes are encountered within the serpentinites which belong to the ophiolitic sequence (Akaad and Abu El Ela, 2002). Sometimes, serpentinite masses include small pockets and veins of magnesite as well as chromitite lenses. The magnesite veins may be formed during the formation of the talc-carbonates.

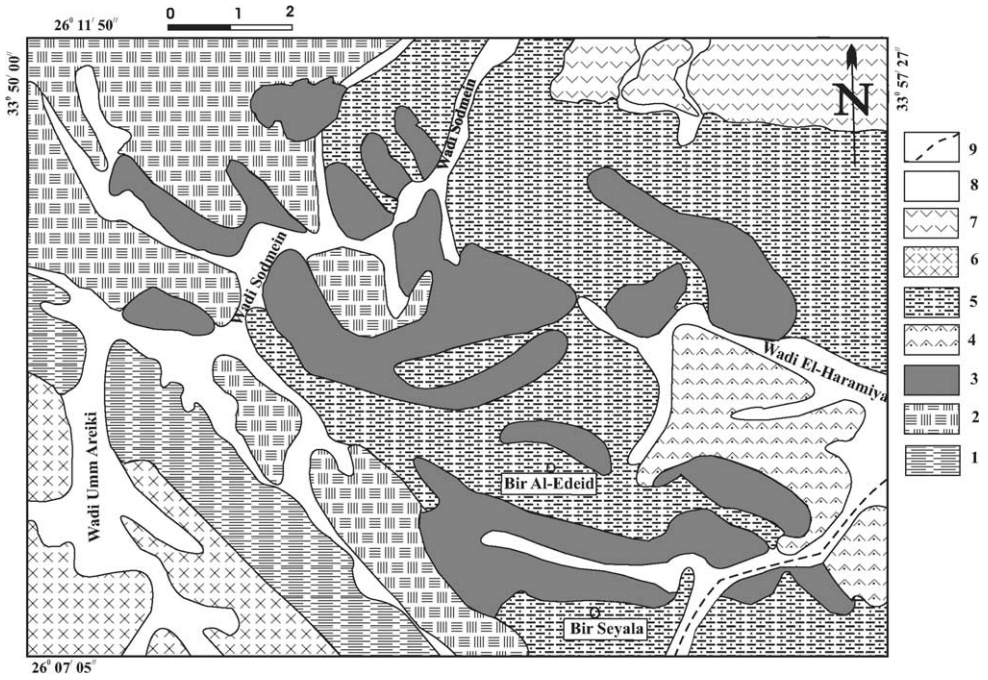

Fig. 2. Geological map of the area around Bir Al-Edeid (modified after Akaad and Abu El Ela, 2002). (1) Meatiq gneisses, (2) Abu Fannani Formation, (3) Serpentinites, (4) Calc-alkaline Metavolcanics, (5) Volcaniclastic metaturbidites, (6) Old granites, (7) Dokhan Volcanics, (8) Wadi deposits and (9) Asphaltic road.

Field studies demonstrate that the serpentinites are sheared and bounded by thrust faults indicating tectonic emplacement. The lack of any thermal effect of studied serpentinites upon the enveloping country rocks, and their occurrence along thrust faults, indicate their tectonic emplacement and excluded the intrusive nature.

4. Petrography

The studied serpentinites include massive and sheared varieties. They are olive green to black coloured fine-grained rocks often mottled with light and dark coloured areas. The green colour of the studied serpentinites is due to its iron content which becomes darker with the increase in the iron content.

4.1. Massive serpentinite

The massive serpentinites are differentiated into serpentinite and partly serpentinized peridotite, besides talc-carbonates and chromitite. The serpentinites are composed essentially of antigorite, chrysotile and lizardite with subordinate amounts of carbonates, chromite, magnetite, magnesite, talc, tremolite and chlorite. *Antigorite* is the most common mineral and occurs as flaky crystals or interpenetrating and interlocking elongate plates. Sometimes, the antigorite flakes and blades are arranged in roughly parallel aggregates. *Chrysotile* occurs as cross-fiber veinlets traversing the antigorite matrix, which indicates its late crystallization under static conditions. *Lizardite* occurs as fine aggregates or as isotropic irregular plates. Magnesite is commonly stained with reddish material (most probably iron oxide) and occurs as granular aggregates and discrete rhombs. Patches of carbonate minerals and opaques as well as chlorite veinlets are present. *Talc* occurs in the groundmass as fine scales and flakes of high interference colours. Sometimes, the serpentine minerals retain the geometric configuration of the original mafic minerals; serpentine developed as an alteration after olivine has a mesh texture while that formed after orthopyroxene has a bastite texture. These textures indicate dunite and harzburgite parent rocks. The opaque minerals in the studied serpentinites (~5–6%) are represented mainly by chromite and magnetite. Chromite occurs as disseminated subhedral crystals and/or irregular grains of reddish brown colour in thin sections, while in the reflected light it is rimmed by magnetite with numerous interstices filled with serpentine minerals. Alteration of chromite along grain borders and cracks is very common. Magnetite occurs as anhedral grains in the interstitial spaces between the serpentine minerals or as vienlets. Sometimes, it is highly martitized.

The partly serpentinized peridotite is composed mainly of antigorite, chrysotile, clinopyroxene relics, chromite and magnetite. The clinopyroxene is represented mainly by augite, which is transformed along its margins and cleavages into serpentines and amphiboles. Talc-carbonates are fine grained and foliated. They are composed mainly of magnesite, talc and less commonly serpentine minerals and chromite. Chromitite lenses are mainly

composed of coarse aggregates of subhedral to anhedral chromite crystals. Few chromite grains show rims of ferritchromite which are highly porous. Intergranular minerals are mainly serpentine and few magnetite grains. The studied chromitite lenses show common textures and structures typical of magmatic crystallization such as cumulate, chain structures and banding (Pal and Mitra, 2004).

4.2. Sheared serpentinite

The sheared serpentinite is less common than the massive type. It has the same composition, but the minerals are commonly arranged in subparallel alignment producing the schistosity. Locally, it is rich in the carbonates, magnesite and chlorite. Chromite is intensively altered, while the magnetite is completely martitized. Late shearing and faulting obliterate the primary textures giving rise to mylonitic, cataclastic and brecciated textures.

5. Mineral chemistry

5.1. Serpentine minerals

Representative analyses of the serpentine minerals are shown in Table 1. Due to different generations of serpentinization, the serpentinite minerals are highly variable in their compositions (Proenza et al., 2004). They contain 42.31–46.46 wt.% SiO_2, 34.89–41.53 wt.% MgO, 0.24–3.36 wt.% Al_2O_3, 0.66–8.26 wt.% FeO and 0.00–1.27 wt.% Cr_2O_3. From Table 1, it is clear that the analyzed chrysotile is richer in SiO_2 and MgO and poorer in FeO than the antigorite, an observation supporting formation of different serpentine generations. According to Coleman (1971), two major petrological types of serpentinites exist. Pseudomorphic serpentinite, which consists dominantly of lizardite with minor concentrations of chrysotile, is generated by retrograde replacement of olivine, orthopyroxene, and clinopyroxene by serpentines. The second type is represented by antigorite serpentinite, which is formed by the recrystallization of pseudomorphic serpentinites during progressive metamorphism. On the MgO versus SiO_2 diagram (Fig. 3A) the analyzed serpentine minerals are mainly antigorite serpentines with subordinate pseudomorphic serpentines, which indicate that the parent minerals were first retrogressed to form lizardite and chrysotile. Progressive metamorphism has recrystallized these minerals into antigorite. The analyzed serpentine minerals are plotted on the Cr_2O_3 versus Al_2O_3 diagram (Fig. 3B) where they show variable contents of Al_2O_3 and Cr_2O_3 corresponding to the composition of Ol-mesh, Opx-bastite and Cpx-bastite serpentines. These features reflect their derivation from dunite and harzburgite. The analyzed serpentine minerals are plotted in the

Table 1
Representative electron microprobe analyses of the serpentine minerals

Mineral	Chrysotile						Antigorite						
Sample No.	1E						2E		3E		4E		
Spot No.	1	2	3	4	5	6	1	2	1	2	1	2	3
Si_2O	46.46	46.31	46.46	45.91	45.80	46.04	43.33	43.60	42.70	42.31	42.89	43.35	43.99
TiO_2	0.01	0.06	0.00	0.00	0.05	0.00	0.06	0.04	0.00	0.01	0.00	0.05	0.00
Al_2O_3	0.29	0.38	0.33	0.31	0.38	0.33	0.35	0.24	1.70	3.36	0.54	0.60	0.79
Cr_2O_3	0.01	0.42	0.01	0.29	0.02	0.03	0.15	0.00	0.65	1.27	0.27	0.38	0.05
MgO	40.80	40.57	40.92	41.21	41.53	41.22	37.66	38.50	36.76	34.89	35.22	35.20	38.91
CaO	0.00	0.01	0.00	0.00	0.01	0.00	0.00	0.03	0.01	0.16	0.07	0.47	0.08
MnO	0.00	0.03	0.21	0.00	0.09	0.00	0.06	0.00	0.05	0.07	0.27	0.22	0.07
FeO	0.66	0.80	0.75	0.83	0.81	0.78	5.04	4.73	5.73	5.76	8.26	7.69	3.64
NiO	0.21	0.21	0.11	0.11	0.08	0.24	0.09	0.04	0.27	0.37	0.03	0.03	0.16
Na_2O	0.00	0.00	0.26	0.00	0.00	0.02	0.00	0.00	0.00	0.02	0.02	0.01	0.00
K_2O	0.00	0.01	0.02	0.01	0.02	0.01	0.01	0.00	0.03	0.02	0.03	0.02	0.02
H_2O	13.26	13.26	13.30	13.25	13.29	13.28	12.66	12.73	12.76	12.80	12.56	12.65	12.89
Total	101.71	101.67	101.94	101.66	102.07	101.94	99.40	99.93	100.65	101.05	100.14	100.67	100.58
Structure formula based on 28 oxygens													
Si	8.40	8.38	8.38	8.31	8.27	8.32	8.21	8.21	8.03	7.93	8.20	8.22	8.18
Ti	0.00	0.01	0.00	0.00	0.01	0.00	0.01	0.01	0.00	0.00	0.00	0.01	0.00
Al	0.06	0.08	0.07	0.07	0.08	0.07	0.07	0.05	0.37	0.74	0.12	0.13	0.17
Cr	0.00	0.01	0.00	0.00	0.00	0.00	0.02	0.00	0.10	0.19	0.04	0.06	0.01
Mg	11.00	10.94	11.00	11.12	11.17	11.10	10.63	10.73	10.29	9.74	10.00	9.92	10.76
Ca	0.00	0.00	0.00	0.00	0.00	0.00	0.00	0.00	0.00	0.03	0.01	0.09	0.01
Mn	0.00	0.00	0.00	0.00	0.01	0.00	0.01	0.00	0.01	0.01	0.04	0.03	0.01
Fe	0.10	0.12	0.11	0.13	0.12	0.12	0.79	0.75	0.90	0.90	1.32	1.22	0.56
Ni	0.03	0.03	0.02	0.02	0.01	0.03	0.01	0.01	0.04	0.05	0.00	0.00	0.02
Na	0.00	0.00	0.01	0.00	0.00	0.01	0.00	0.00	0.00	0.01	0.00	0.00	0.00
K	0.00	0.00	0.00	0.00	0.00	0.00	0.00	0.00	0.01	0.00	0.00	0.00	0.00

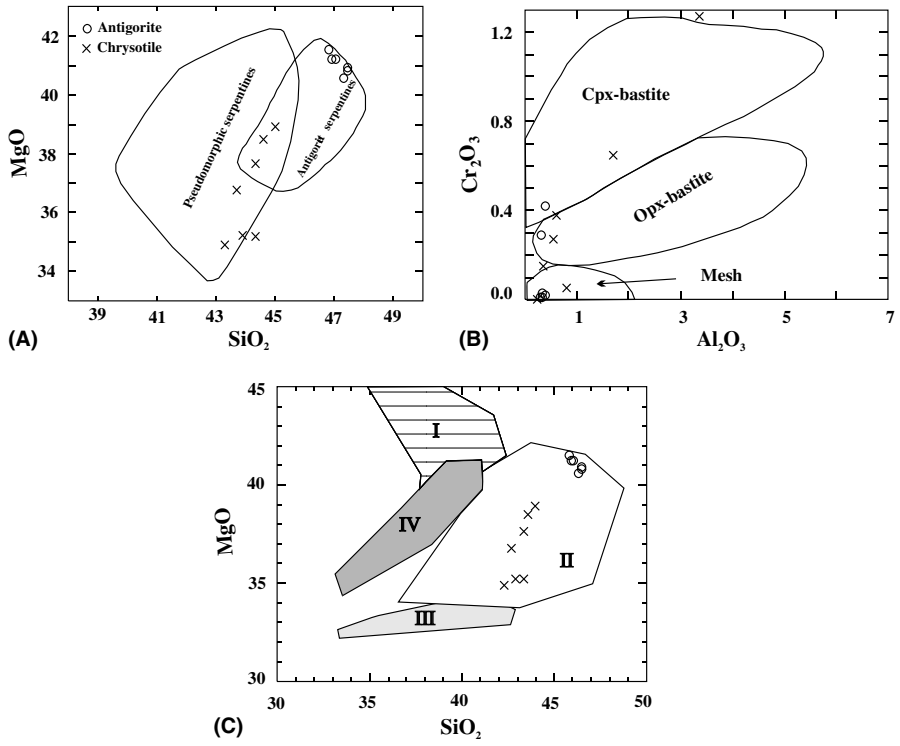

Fig. 3. (A) MgO versus SiO_2 for the analyzed serpentine minerals (adapted from Dungan, 1979). (B) Cr_2O_3 versus Al_2O_3 for the analyzed serpentine minerals (adapted from Dungan, 1979). (C) MgO versus SiO_2 for the analyzed serpentine minerals (Wicks and Plant, 1979). I: Lizardite after magmatic olivine, II: Antigorite with interpeatratig texture, III: Antigorite with hourglass texture, IV: Lizardite after metamorphic olivine.

Table 2
Representative electron microprobe analyses of chromite from the serpentinites

Sample No.	1S				1E			
Spot No.	1	2	3	4	1	2	3	
							Core	Rim
Si_2O	0.02	0.00	0.00	0.00	0.03	0.00	0.02	0.01
TiO_2	0.16	0.09	0.09	0.10	0.12	0.10	0.13	0.28
Al_2O_3	12.32	14.83	13.50	13.43	15.97	14.41	13.96	9.97
Cr_2O_3	56.35	56.38	56.96	57.26	55.45	54.53	54.02	58.45
Fe_2O_3	3.96	4.26	3.36	3.89	3.02	2.96	3.89	2.96
MgO	15.25	14.17	13.83	13.78	13.98	14.41	14.35	9.98
CaO	0.03	0.02	0.00	0.01	0.00	0.03	0.00	0.02
MnO	0.41	0.34	0.43	0.34	0.35	0.31	0.38	0.35
FeO	11.57	9.92	11.79	11.00	11.31	12.07	13.21	18.10
NiO	0.12	0.06	0.16	0.09	0.11	0.06	0.09	0.17
ZnO	0.01	0.00	0.00	0.04	0.00	0.07	0.00	0.01
Total	100.20	100.06	100.12	99.96	100.33	98.96	100.06	100.30
Structure formula based on 32 oxygens								
Si	0.005	0.000	0.000	0.000	0.007	0.000	0.005	0.003
Ti	0.030	0.017	0.017	0.020	0.022	0.020	0.025	0.055
Al	3.675	4.371	4.027	4.006	4.688	4.285	4.266	3.098
Cr	11.279	11.150	11.396	11.457	10.921	10.881	11.074	12.194
Fe^{3+}	0.755	0.800	0.639	0.735	0.566	0.561	0.252	0.587
Mg	5.801	5.331	5.259	5.239	5.231	5.463	5.590	3.956
Ca	0.008	0.006	0.000	0.003	0.000	0.271	0.000	0.006
Mn	0.088	0.072	0.093	0.073	0.073	0.067	0.084	0.078
Fe^{2+}	2.445	2.071	2.491	2.324	2.351	2.541	2.859	3.986
NiO	0.024	0.012	0.032	0.018	0.022	0.012	0.019	0.036
Zn	0.002	0.000	0.000	0.008	0.000	0.014	0.000	0.002
Cr#	0.75	0.72	0.74	0.74	0.70	0.72	0.72	0.80
Mg#	0.70	0.72	0.68	0.69	0.69	0.68	0.66	0.50
Fe^{3+}#	0.06	0.07	0.05	0.06	0.05	0.05	0.02	0.05

field characteristic for prograde metamorphism (Fig. 3C) in which antigorite with interpenetrating texture is formed at low temperature (Wicks and Plant, 1979).

5.2. Chromite

Only the primary chromite crystals were selected for analysis, while the altered and metamorphosed chromites are eliminated. Representative analyses for the primary chromite crystals are given in Table 2. In the completely serpentinized ultramafic rocks containing no relicts of primary silicate minerals, the composition of the unaltered accessory chromite is extensively used as a petrogenetic and geotectonic indicator (Irvine, 1967; Dick and Bullen, 1984; Arai, 1992). Chromite is the only igneous mineral that retains most of its original igneous chemistry in metamorphosed serpentinites (Bames, 2000; Proenza et al., 2004).

The analyzed chromite crystals have uniform composition, except one crystal having a ferritchromite rim (up to 18.10 wt.% FeO). They have high Cr# and Mg# representing most probably the primary phase which is similar to chromian spinels in mantle-derived peridotites (Roeder, 1994). Also, the analyzed chromites have Fe^{3+}# less than 0.1 and low TiO_2 content (<0.28 wt.%) which are similar to podiform chromite (Leblanc et al., 1980). They are low in Al relative to Cr and are similar to ophiolitic podiform chromite particularly to those associated with harzburgite (Fig. 4A–C).

5.3. Pyroxene

The chemical analyses of the pyroxene relics from partly serpentinized peridotites are represented in Table 3. According to Morimoto et al. (1988), the analyzed pyroxenes are mostly augite (Fig. 5). The analyzed clinopyroxene has $TiO_2 < 1.0\%$ which is characteristic for non-alkaline rocks (Le Bas, 1962). It shows a narrow compositional range of Mg# (0.83–0.86) as well as TiO_2 (0.62–0.77 wt.%), Al_2O_3 (2.92–3.97 wt.%), Cr_2O_3 (0.48–1.07 wt.%), MgO (16.14–17.17 wt.%) and CaO (19.11–20.64 wt.%) contents. These ranges lie within or near the rages of values for mantle derived ultramafic xenoliths at Canary Island (Abu El-Rus et al., in press), which have a Mg# of 0.77–0.96 and 0.01–4.21 wt.% TiO_2, 0.71–11.97 wt.% Al_2O_3, 0.14–2.43 wt.% Cr_2O_3, 11.98–20.38 wt.% MgO and 19.27–24.34 wt.% CaO contents. The tectonic setting of the analyzed clinopyroxenes is deduced from F_1–F_2 discrimination diagram (not shown here) of Nisbet and Pearce (1977), which indicates an ocean-floor tectonic setting.

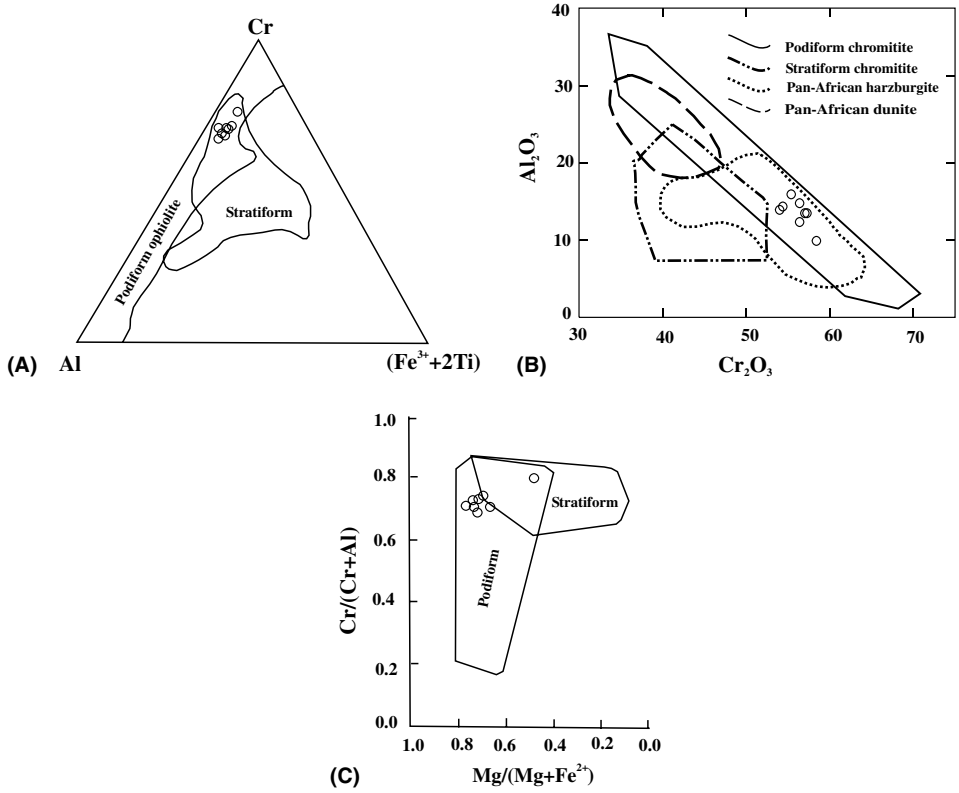

Fig. 4. (A) Cr–(Fe^{3+} + 2Ti)–Al diagram for the analyzed accessory chromite (Jan and Windley, 1990). (B) Al_2O_3 versus Cr_2O_3 for the analyzed accessory chromite (Bonavia et al., 1993). (C) Cr/(Cr + Al) versus Mg/(Mg + Fe^{2+}) for the analyzed chromite (Irvine, 1967; Leblanc and Nicolas, 1992).

Table 3
Electron microprobe analyses of clinopyroxenes

Sample No.	6E			18E	
Spot No.	1	2	3	1	2
Si_2O	52.098	52.010	52.550	51.880	51.670
TiO_2	0.766	0.650	0.660	0.700	0.620
Al_2O_3	3.970	3.110	2.920	3.350	3.140
Cr_2O_3	1.068	0.525	0.523	0.578	0.478
MgO	16.366	16.570	17.170	16.140	16.240
CaO	19.143	20.640	19.110	20.390	20.620
MnO	0.166	0.131	0.129	0.165	0.124
FeO	6.008	5.400	5.119	5.433	5.032
Na_2O	0.930	0.422	0.358	0.397	0.434
K_2O	0.216	0.027	0.000	0.006	0.038
Total	100.731	99.485	98.539	99.039	98.396
Structure formula based on 6 oxygens					
Si	1.918	1.911	1.945	1.924	1.918
Al^{IV}	0.082	0.089	0.055	0.076	0.082
Al^{VI}	0.090	0.046	0.073	0.070	0.056
Cr	0.031	0.015	0.015	0.017	0.014
Mg	0.899	0.856	0.948	0.835	0.837
Ca	0.755	0.855	0.758	0.849	0.874
Mn	0.002	0.004	0.004	0.005	0.004
Fe	0.185	0.166	0.159	0.169	0.157
Ti	0.021	0.025	0.018	0.025	0.026
Na	0.016	0.030	0.026	0.029	0.031
K	0.001	0.001	0.000	0.000	0.002
Wo	41.030	45.440	40.570	45.700	46.680
En	48.810	45.490	50.720	44.920	44.730
Fs	10.160	9.070	8.710	9.380	8.590
F_1	−0.796	−0.796	−0.778	−0.798	−0.793
F_2	−2.509	−2.465	−2.502	−2.475	−2.444

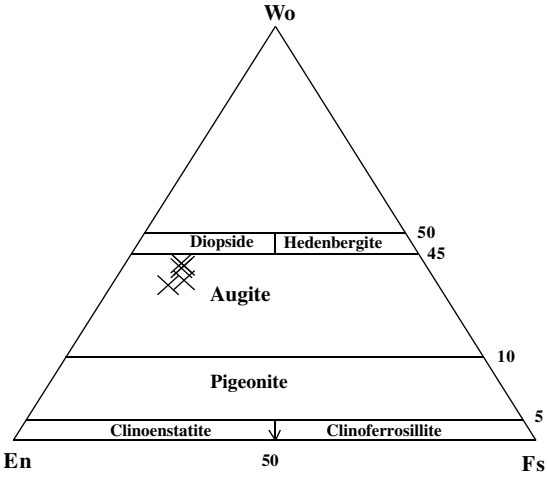

Fig. 5. Composition of the analyzed clinopyroxenes in the partly serpentinized rocks (Morimoto et al., 1988).

6. Geochemistry

6.1. Geochemical characteristics

Representative chemical analyses and calculated normative minerals of the massive serpentinites are given in Table 4. Unfortunately, the concentrations of some elements such as Y, Nb, Rb and Ba are below the detection limits. Also, the chemical analyses of the chromitite are given in Table 5. The analyzed serpentinites show a wide variation in SiO_2 (34.40–45.39 wt.%), MgO (34.27–41.39 wt.%), FeO (3.59–8.18 wt.%) and narrow ranges in the other elements. Cr and Ni contents are high (1184–3442 ppm and 1878–5045 ppm, respectively), while Co ranges from 92 to 202 ppm. The high concentrations of Cr and Ni in the analyzed serpentinites reflect their development from a depleted-mantle peridotite source. The partly serpentinized rocks (sample nos. 6E and 18E) are similar in their composition to the highly serpentinized rocks, but they are rich in CaO. The studied serpentinites have Ni/Co ratios ranging between 18.63 and 32.40 with an average ratio of 24.19, which are very close to that of Alpine-type peridotites (Gulacar and Delalaye, 1976). Moreover, all the analyzed serpentinites have MgO/$\sum$FeO ratios <12 which are characteristic for the Alpine type ultramafic magma series (Hess, 1938).

The $MgO/MgO + FeO^{2+}$ ratios of the analyzed serpentinites range from 0.83 to 0.92 with an average of 0.86. This average is similar to that of the metamorphic dunites (0.86) and is generally close to the average ratio for the metamorphic lherzolites (0.84) and metamorphic harzburgites (0.85) given by Coleman (1977). Olivine, orthopyroxene and clinopyroxene normative compositions are calculated and plotted on the Ol–Cpx–Opx diagram of Coleman (1977), where the highly serpentinized rocks fall within the harzburgite field (except sample no. 10E which falls in the dunite field), while the partly serpentinized rocks plot in the wehrlite field (Fig. 6A). The analyzed serpentinites are plotted within the field of metamorphic peridotites associated with ophiolites (Fig. 6B and C).

The analyzed chromitite has high Cr_2O_3, Fe_2O_3, Al_2O_3 and MgO contents. It is rich in Co, Ni, V and Zn and depleted in Rb, Ba, Sr, Zr and Nb. The chemical analyses of the chromitite lenses suggest a podiform Alpine-type chromite, as the latter has $Cr_2O_3 < 50$ wt.%, $FeO_{(t)} <$ 20 wt.%, $TiO_2 < 0.3$ wt.% and MnO <1 wt.% (Dickey, 1975; Jan and Windley, 1990).

6.2. Tectonic setting

The petrographical and geochemical investigations indicate that the studied serpentinites were formed mainly after harzburgite and less commonly after dunite and wehrlite. According to Berhe (1990), the Pan-African ophiolites in NE and E Africa are of back-arc or supra-subduction origin. Floyd (1991) distinguished the tectonic setting of the peridotite on petrological and geochemical grounds into: (1) rift to passive margin peridotites, (2) mid-ocean ridge peridotites, (3) intra-plate peridotites, and (4) active margin peridotites. Also, Bonatti and Michael (1989) distinguished between peridotites of different tectonic setting based on Al_2O_3 content in the whole-rock and mineral chemistry because Al appears to be relatively unaffected by serpentinization and metamorphism. Al_2O_3 content in the peridotites decreases from intracontinental (pre-oceanic) rifts to

Table 4
Major oxides, calculated normative minerals and trace elements (in ppm) for the studied serpentinites

	1E	2E	3E	4E	7E	8E	9E	10E	11E	12E	14E	1S	2S	6E[a]	18E[a]
Si_2O	35.92	38.20	39.90	37.04	38.99	37.44	40.98	34.43	38.20	39.18	42.72	34.40	35.87	36.35	45.39
TiO_2	0.02	0.01	0.04	0.01	0.01	0.01	0.02	0.01	0.01	0.01	0.01	0.02	0.01	0.02	0.02
Al_2O_3	0.49	0.57	1.37	0.83	0.77	1.58	0.42	0.67	0.56	0.67	0.67	0.49	0.48	0.90	0.38
Fe_2O_3	1.96	1.84	2.22	2.18	1.71	1.74	1.80	2.24	2.07	1.69	1.20	1.79	1.70	1.65	1.73
FeO	6.89	6.13	7.27	7.47	5.60	5.87	5.63	8.18	6.90	5.53	3.59	6.53	5.97	5.72	4.92
MnO	0.09	0.08	0.10	0.09	0.24	0.12	0.10	0.32	0.14	0.15	0.14	0.11	0.16	0.15	0.11
MgO	36.72	36.54	35.18	39.21	39.12	38.14	35.77	40.27	38.07	41.39	40.37	35.12	40.13	38.11	34.27
CaO	0.30	0.71	0.15	0.52	0.29	0.69	0.09	0.29	0.29	0.13	0.27	0.08	0.20	2.04	1.27
Na_2O	0.04	0.09	0.13	0.08	0.37	0.35	0.06	0.08	0.10	0.08	0.05	0.04	0.03	0.32	0.04
K_2O	0.01	0.01	0.03	0.01	0.02	0.03	0.01	0.01	0.02	0.01	0.02	0.01	0.01	0.07	0.01
P_2O_5	0.01	0.01	0.03	0.01	0.05	0.04	0.01	0.03	0.02	0.01	0.02	0.01	0.01	0.03	0.01
LOI	16.77	14.12	12.60	12.30	11.20	12.00	13.20	12.20	11.90	11.10	10.20	21.19	15.05	14.50	11.20
Total	99.22	98.31	99.02	99.75	98.37	98.01	98.09	98.73	98.28	99.95	99.26	99.79	99.62	99.86	99.35
Normative minerals															
C	0.00	0.00	1.08	0.00	0.00	0.00	0.20	0.08	0.00	0.35	0.14	0.37	0.09	0.00	0.00
Or	0.07	0.07	0.21	0.07	0.14	0.21	0.07	0.07	0.14	0.07	0.13	0.08	0.07	0.48	0.07
Ab	0.41	0.90	1.29	0.77	3.63	3.44	0.60	0.78	0.98	0.76	0.48	0.43	0.30	3.17	0.38
An	1.37	1.33	0.64	2.15	0.44	3.08	0.45	1.44	1.18	0.65	1.36	0.42	1.10	0.95	0.94
Di	0.28	2.18	0.00	0.58	0.67	0.47	0.00	0.00	0.26	0.00	0.00	0.00	0.00	8.39	4.82
Hy	21.47	28.12	35.91	13.93	19.44	13.47	47.17	0.99	24.15	21.23	39.60	23.49	12.56	1.52	60.73
Ol	72.88	64.17	56.98	78.84	74.33	76.21	48.39	92.79	69.74	74.13	56.27	71.83	82.92	82.55	30.14
Mt	3.45	3.17	3.77	3.61	1.19	2.93	3.07	3.75	3.47	2.76	1.95	3.30	2.91	2.80	2.85
Il	0.05	0.02	0.04	0.02	0.02	0.09	0.02	0.02	0.02	0.02	0.02	0.05	0.02	0.04	0.04
Ap	0.03	0.03	0.08	0.03	0.14	0.11	0.03	0.08	0.05	0.03	0.05	0.03	0.03	0.08	0.03
Trace elements (in ppm)															
Co	93	92	160	149	174	114	179	171	170	168	135	108	92	202	142
Cr	2458	2343	2621	3442	2491	1451	1569	3148	1759	3346	1184	2368	1995	2265	1484
Ni	1978	1878	3670	3960	3929	2900	4597	4353	3622	3316	4117	2013	2981	5045	3607
Ga	3	4	5	3	4	3	3	4	3	4	3	4	3	4	5
Sr	10	13	23	11	12	13	13	26	10	14	12	2	5	18	10
V	36	46	45	34	34	38	40	35	46	36	38	30	31	46	37
Zn	37	37	34	39	36	34	38	35	36	35	37	34	36	37	34
Zr	8	12	9	12	10	14	18	12	9	16	16	10	7	12	13
Ba	<10	<10	<10	<10	<10	<10	<10	<10	<10	<10	<10	<10	<10	<10	<10
Rb	<2	<2	<2	<2	<2	<2	<2	<2	<2	<2	<2	<2	<2	<2	<2
Y	<2	<2	<2	<2	<2	<2	<2	<2	<2	<2	<2	<2	<2	<2	<2
Nb	<2	<2	<2	<2	<2	<2	<2	<2	<2	<2	<2	<2	<2	<2	<2

[a] Partly serpentinized rocks.

Table 5
Chemical analyses for the chromitite

	1S	2S
Si_2O	6.34	5.04
TiO_2	0.09	0.1
Al_2O_3	16.77	13.12
Fe_2O_3	14.13	18.07
Cr_2O_3	38.76	40.48
MnO	0.16	0.21
MgO	21.14	19.61
CaO	0.13	0.38
Na_2O	0.01	n.d.
K_2O	n.d.	n.d.
P_2O_5	0.01	0.01
LOI	2.09	2.59
Total	99.63	99.61
Trace elements (in ppm)		
Co	187	214
Ni	1512	1443
Ga	19	18
Sr	2	5
V	725	865
Zn	250	361
Zr	2	3
Ba	12	19
Rb	2	2
Y	3	5
Nb	3	4

passive margins to mature ocean to subduction zones. The studied serpentinites have low concentrations of Al_2O_3 (0.38–1.58 wt.%). Also, the most depleted peridotites are found in supra-subduction zone environments. The analyzed serpentinites as well as the Pan-African serpentinites in the Eastern Desert of Egypt are similar to active margin peridotites, e.g., from Tonga and Puerto Rico (Fig. 7A). Most of the analyses plot within the supra-subduction zone ophiolite field on the Cr versus TiO_2 diagram (Fig. 7B) of Pearce et al. (1984). The TiO_2 versus Cr# of the analyzed accessory chromite mineral plot in the depleted mantle peridotite field, close to the boninite field (Fig. 7C), indicating a supra-subduction setting (Berhe, 1990). Moreover, the presence of podiform chromites in the studied serpentinites is considered to be typical of supra-subduction ophiolites (Kröner et al., 1987). The analyzed chromitite has Cr_2O_3 (<50 wt.%) and TiO_2 (<0.3 wt.%) contents similar to the depleted upper mantle source (Jan and Windley, 1990).

7. Discussion and conclusions

The investigated serpentinites occur as isolated masses, imbricate slices of variable thicknesses and as small blocks or lenses incorporated in the sedimentary matrix of the mélange. They are mainly thrust over the associated island arc calc-alkaline metavolcanics. The serpentinites are generally massive but become progressively foliated along thrust faults. Along shear zones, they are commonly replaced by talc-carbonates probably due to CO_2-metasomatism. Serpentinite masses contain small lenses of chromitite, pockets and veins of magnesite, and cut by pyroxenite dykes. The studied serpentinites are distinguished into (a) completely serpentinized rocks, and (b) partly serpentinized rocks containing relicts of the original mafic minerals (clinopyroxene). Lack of thermal effect of the studied serpentinites upon the enveloping country

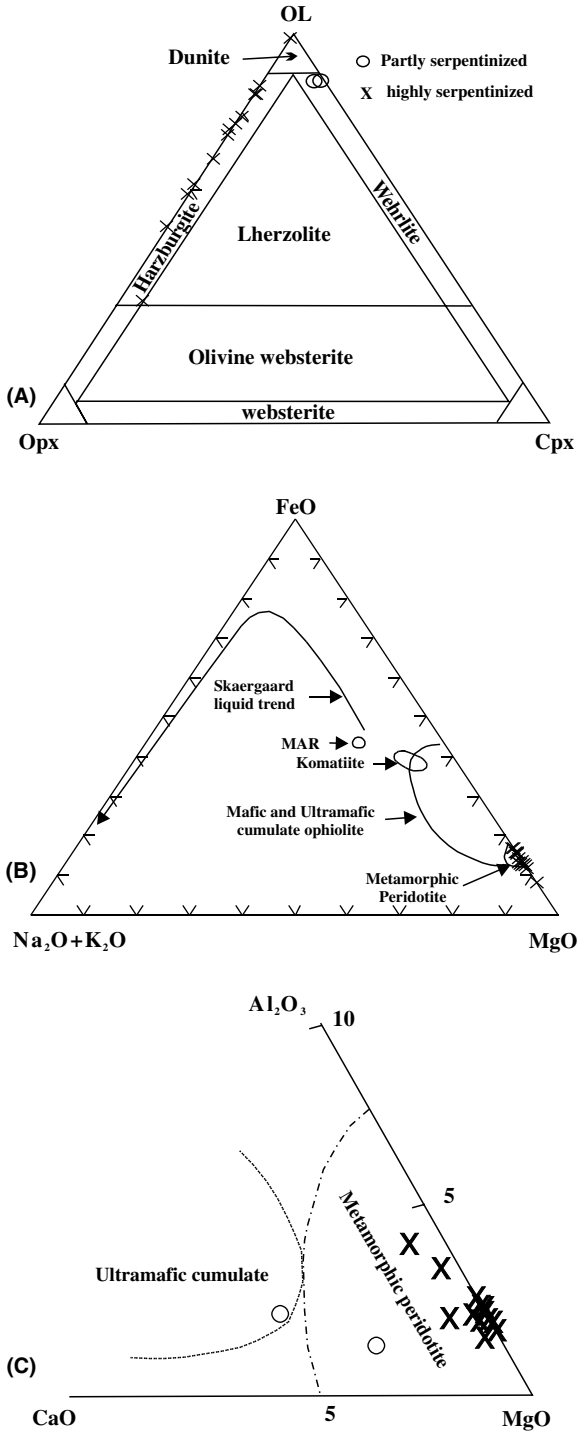

Fig. 6. (A) Ol–Cpx–Opx normative composition of the studied serpentinites (Coleman, 1977). (B) FeO–MgO–($Na_2O + K_2O$) diagram for the studied serpentinites (Coleman, 1977). (C) Al_2O_3–MgO–CaO diagram for the studied serpentinites (Coleman, 1977).

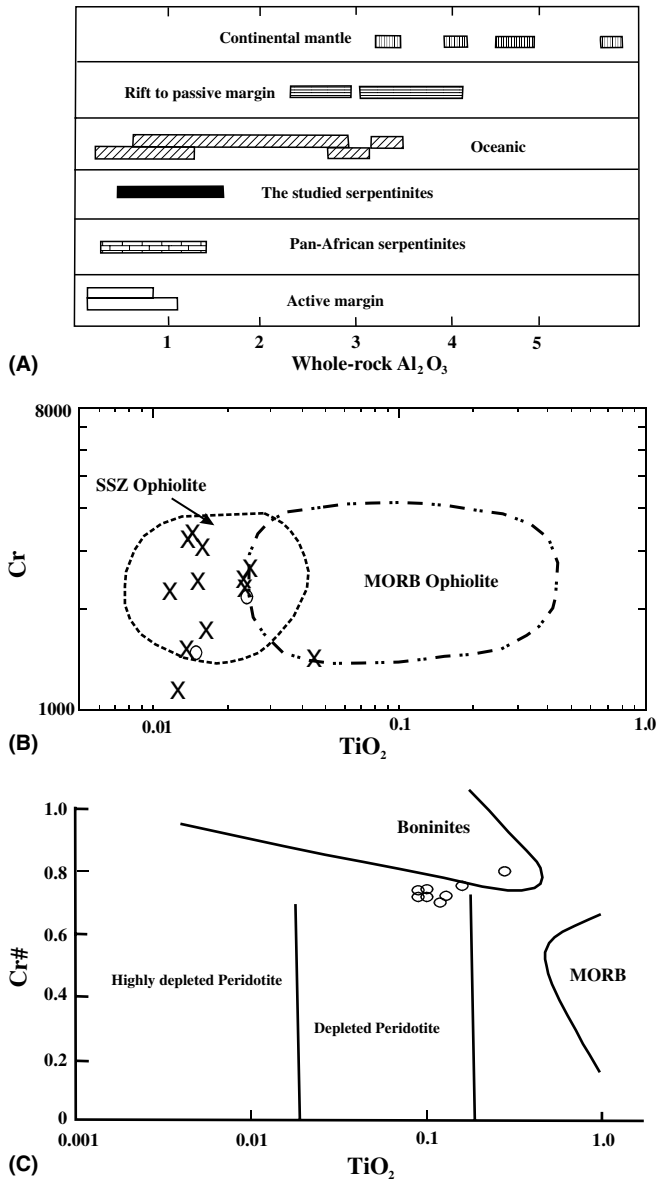

Fig. 7. (A) Al_2O_3 contents of the whole-rock of the studied serpentinites compared with those from other tectoic settings (from Floyd, 1991). The Al_2O_3 of the Pan-African serpentinites adopted from El Bahariya and Arai (2003). (B) Cr versus TiO diagram for the studied serpentinites (Pearce et al., 1984). (C) Cr# versus TiO diagram for the analyzed accessory chromite (fields after Dick and Bullen, 1984; Arai, 1992; Jan and Windley, 1990).

rocks, as well as their association with thrust faults indicates their tectonic emplacement.

Petrographically, the highly serpentinized masses consist mainly of antigorite with variable amounts of lizardite, chrysotile, magnetite, chromite, magnesite, talc, chlorite and tremolite. The partly serpentinized rocks have the same composition as the highly serpentinized rocks in addition to the presence of original clinopyroxene relics. The predominance of antigorite over other serpentine minerals indicates that the present serpentinites have undergone prograde metamorphism or the parent ultramafic rocks were serpentinized under higher pressure (Faust and Fahey, 1962; Yoder, 1967; Moody, 1976; Deer et al., 1992), most probably during their tectonic emplacement onto the continental margin. The presence of chrysotile as cross-fiber vienlets cutting across the other serpentine minerals indicates a late genesis as a result of the activity of meteoric waters. The studied serpentinites have been derived from harzburgite and dunite due to the prevalence of mesh and bastite textures.

The analyzed serpentine minerals show a wide variation in SiO_2, MgO, Al_2O_3, FeO and Cr_2O_3 probably due to the presence of different serpentine generations. The chemical characteristics of the primary chromite from the studied serpentinites are similar to those of podiform ophiolitic chromites. Sometimes, it is altered along the peripheries into magnetite and ferritchromite due to serpentinization and prograde metamorphism (Bliss and Maclean, 1975). The Cr# of the accessory chromite in the ultramafic rocks has been used as an indicator of the degree of melting in the upper mantle; high-Cr chromites correlate with the highest degree of melting and the greater degree of depletion of the peridotite (Dick and Bullen, 1984; Arai, 1992). The serpentinites have accessory chromites with high Cr# (0.70–0.80) which reflects an increase in the degree of partial melting and a depleted upper mantle source. The analyzed pyroxene relicts are augite which is nearly similar to those in Wadi Ghadir ophiolite (Basta and Hafez, 1985). The chemical compositions of the analyzed clinopyroxene indicate that the original parent magma was subalkaline in nature.

The talc carbonates formed at the expense of previously serpentinized rocks along shear zones during late stage CO_2-metasomatism. The serpentinites have suffered regional metamorphism up to the greenschist facies, which occurred during the collisional stage or back-arc basin closure, followed by thrusting over a continental margin. Geochemically, they are relatively rich in MgO, Cr, Ni and Co indicating derivation from harzburgites together with minor dunites and wehrlites. The studied serpentinites show similarities to the Alpine-type serpentinites. They represent a fragment of oceanic lithosphere that has been formed in a back-arc environment; i.e., they belong to an ophiolitic mantle sequence formed in a supra-subduction zone. Chromite, magnesite and talc represent the mineral deposits associated with the serpentinites in the studied area. The authors recommend more detailed study of the mineral deposits associated with the serpentinites in the present area.

Acknowledgement

The authors are greatly indebted to Prof. El-Gaby for his fruitful discussions and valuable comments.

References

Abu El Ela, A.M., 1996. Contribution to mineralogy and geochemistry of some serpentinites from the Eastern Desert of Egypt. M.E.R.C. Ain Shams University. Earth Science 10, 1–25.

Abu El-Rus, M.A., Neumann, E.R., Peters, V., in press. Serpentinization and dehydration in the upper mantle beneath Fuerteventura (Eastern Canary Island); Evidence from mantle xenoliths. Egyptian Mineralogist.

Ahmed, A.A., 1983. Ultrabasic intrusions in the Eastern Desert, Egypt. International Basement Tectonic Association 5, 68–75.

Ahmed, A.A., 2005. The status of uncertain "ophiolites" in the Eastern Desert of Egypt. In: 1st Symposium on the Classification of the Basement Complex of Egypt, pp. 52–61.

Akaad, M.K., 1996. Rock succession of the Basement: An autobiography and assessment. Geological Survey of Egypt, Paper No. 71.

Akaad, M.K., 1997. On the behavior of serpentinites and its implications. Geological Survey of Egypt, Paper No. 74.

Akaad, M.K., Abu El Ela, A.M., 2002. Geology of the basement rocks in the eastern half of the belt between latitudes 25°30′ and 26°30′N Central Eastern Desert, Egypt. Geological Survey of Egypt, Paper No. 78.

Akaad, M.K., El Ramly, M.F., 1961. Geological history and classification of the basement rocks of the central Eastern Desert of Egypt. Geological Survey of Egypt, Paper No. 9.

Akaad, M.K., Noweir, A.M., 1972. Some aspects of the serpentinites and their associated derivations along Qift-Quseir road, Eastern Desert. Annals of the Geological Survey of Egypt 2, 251–270.

Akaad, M.K., Noweir, A.M., 1980. Geology and Lithostratigraphy of the Arabian Desert orogenic belt of Egypt between Lat. 25°35′ and 26°30′N. Bulletin of the Institute of Applied Geology, King Abdul Aziz University, Jeddah 3 (4), 127–135.

Arai, S., 1992. Chemistry of chromian spinel in volcanic rocks as a potential guide to magma chemistry. Mineralogical Magazine 56, 173–184.

Asran, A.M.H., Kabesh, M.L., 2003. Petrology, geochemistry and opaques of mélange rocks along Wadi Abu Haramiya, central Eastern Desert, Egypt. In: 5th International Conference of the Geology of the Middle East, Cairo, pp. 155–173.

Asran, A.M.H., Azer, M.K., Aboazom, A.S., 2005. Petrological and geochemical investigations on Dokhan Volcanics and felsites in Wadi Sodmein area, central Eastern Desert, Egypt. Egyptian Journal of Geology 49 (1).

Bames, S.J., 2000. Chromite in Komatites, II. Modification during greenschist to mid-amphibolite facies metamorphism. Journal of Petrology 41, 387–409.

Basta, E.Z., Abdel Kader, Z., 1969. The mineralogy of Egyptian serpentinites and talc-carbonates. Mineralogical Magazine 37, 394–408.

Basta, F.F., Hafez, A.M., 1985. Clinopyroxenes as petrogenetic indicators in the Egyptian Proterozoic rocks. Neues Jahrbuch für Mineralogie 153, 77–90.

Basta, E.Z., Hanafy, M.A., 1971. Alteration of some Egyptian chromites. Proceeding of the Egyptian Academy of Science 22, 1–8.

Berhe, S.M., 1990. Ophiolites in Northeast and East Africa: implications for Proterozoic crustal growth. Journal of the Geological Society London 147, 41–57.

Bliss, N.W., Maclean, W.H., 1975. The paragenesis of zoned chromite from central Manitoba. Geochimica et Cosmochimica Acta 39, 973–990.

Bonatti, E., Michael, P.J., 1989. Mantle peridotites from continental rifts to oceanic basins to subduction zones. Earth and Planetary Science Letters 91, 297–311.

Bonavia, F.F., Diella, V., Ferrario, A., 1993. Precambrian podiform chromitites from Kenticha Hill, southern Ethiopia. Economic Geology 88, 198–202.

Coleman, R.G., 1971. Plate tectonic emplacement of upper mantle peridotite along continental edges. Journal of Geological Research 76, 1212–1222.

Coleman, R.G., 1977. Ophiolites. Springer-Verlag, Berlin, 229 pp.

Deer, W.A., Howie, R.A., Zussman, J., 1992. An introduction to the rock forming minerals, second ed. Longman Scientific and Technical, London, 696 pp.

Dick, H.B., Bullen, T., 1984. Chromian spinel as a petrogenetic indicator in abyssal and Alpine-type peridotites and spatially associated lavas. Contribution to Mineralogy and Petrology 86, 54–76.

Dickey Jr., J.S., 1975. A hypothesis of origin for podiform chromite deposits. Geochimica et Cosmochimica Acta 39, 1061–1074.

Dungan, M.A., 1979. A microprobe study of antigorite and some serpentine pseudomorphs. Canadian Mineralogist 17, 711–784.

El Bahariya, G.A., Arai, S., 2003. Petrology and origin of Pan-African serpentinites with particular reference to chromain spinel composition, Eastern Desert, Egypt: Implication for supra-subduction zone ophiolite. In: 3rd International Conference on the Geology of Africa, Assiut University, Egypt, pp. 371–388.

El Gaby, S., 1984. Geology and tectonic framework of the Pan-African orogenic belt in Egypt. In: Proceedings of the Second International Conference on Geology of the Arab World, Cairo University (Abstract).

El Gaby, S., El-Nady, O., Khudeir, A.A., 1984. Tectonic evolution of the basement complex in the Central Eastern Desert of Egypt. Geological Rundschau 73, 1019–1036.

El Gaby, S., List, F.K., Tehrani, R., 1988. Geology, evolution and metallogenesis of the Pan-African Belt in Egypt. In: El Gaby, S., Greiling, R.O. (Eds.), The Pan-African Belt of Northeast Africa and Adjacent Areas. Viewig, Braunschweig, pp. 17–68.

El Ramly, M.F., 1972. A new geological map for the basement rocks in the Eastern and Southwestern Deserts of Egypt. Annals of the Geological Survey of Egypt II, 1–18.

El Sharkawy, M.A., El Bayoumi, R.M., 1979. The ophiolites of Wadi Ghadir area, Eastern Desert, Egypt. Annals of the Geological Survey of Egypt 9, 125–135.

Faust, G.T., Fahey, J.J., 1962. The serpentinite-group minerals. United Stated Geological Survey, Professional Paper 384, pp. 1–92.

Floyd, P.A., 1991. Oceanic basalts. Blachie and Son Ltd, 455 pp.

Gulacar, O.F., Delalaye, M., 1976. Geochemistry of nickel, cobalt and copper in Alpine-type ultramafic rocks. Chemical Geology 17, 269–280.

Habib, M.E., 1987. Arc-ophiolites in the Pan-African basement between Meatiq and Abu Furad, Eastern Desert, Egypt. Bulletin Faculty of Science, Assiut University 16, 241–283.

Habib, M.E., Ahmed, A.A., El-Nady, O., 1985. Two orogenics in the Meatiq area of the CED, Egypt. Precambrian Research 30, 83–111.

Hess, H.H., 1938. A primary peridotite magma. American Journal of Science 35, 321–344.

Irvine, T.N., 1967. Chromian spinel as a petrogenetic indicator; Part II. Petrologic applications. Canadian Journal of Earth Sciences 4, 71–103.

Jan, M.Q., Windley, B.F., 1990. Chromian spinel-silicate chemistry in ultramafic rocks of the Jijal complex, Northwestern Pakistan. Journal of Petrology 31, 667–715.

Kröner, A., Greiling, R., Reischman, T., Hussein, I.M., Stern, R.J., Durr, S., Kruger, R., Zimmer, M., 1987. Pan-African crustal evolution in the Nubian segment of Northeast Africa. In: Kröner, A. (Ed.), Proterozoic Lithosphere Evolution, Geodynamics Series. International Lithosphere Program contribution, vol. 17. American Geophysical Union, Washington, pp. 235–257.

Le Bas, M.J., 1962. The role of aluminum in igneous clinopyroxenes with relation to their parentage. American Journal of Science 260, 267–288.

Leblanc, M., Nicolas, A., 1992. Les chromitites ophiolitiques. Chronique de la Recherche Minière 507, 3–25.

Leblanc, M., Dupuy, C., Cassard, D., Noutte, J., Nicolas, A., 1980. Essai sur la genese des corps podiformes de chromite dans les peridotites ophiolitiques: etude des chromites de Nouvelle. In: Panayiotou, A. (Ed.), Ophiolites Proceedings International Symposium Cyprus. Geological Survey Department, Cyprus Publication, pp. 691–701.

Moody, J.B., 1976. Serpentinization: A review. Lithos 9, 125–138.

Morimoto, N., Fabries, J., Ferguson, A.K., Ginzburg, I.V., Ross, M., Seifert, F.A., Zussman, J., 1988. Nomenclature of pyroxenes. Mineralogical Magazine 52, 535–550.

Nisbet, E.G., Pearce, J.A., 1977. Clinopyroxene composition in mafic lavas from different tectonic settings. Contribution to Mineralogy and Petrology 63, 149–160.

Pal, T., Mitra, S., 2004. P–T–fO_2 controls on a partly inverse chromite-bearing ultramafic intrusive: an evaluation from the Sukinda Massif, India. Journal of Asian Earth Sciences 22, 483–493.

Pearce, J.A., Lippard, S.J., Roberts, S. 1984. Characteristics and tectonic significance of supra-subduction zone ophiolites. In: Kokelaar, B.P., Howells, M.F. (Eds.), Marginal Basin Geology. Geological Society, Special Publication, vol. 16, pp. 77–94.

Proenza, J.A., Ortega-Gutierrez, F., Camprubi, A., Tritlla, J., Elias-Herrera, M., Reyes-Salas, M., 2004. Paleozoic serpentinites enclosed chromitites from Tehuitzingo (Acatlán Complex, southern Mexico): a petrological and mineralogical study. Journal of South American Earth Sciences 16, 649–666.

Ries, A.C., Shackleton, R., Graham, R.H., Fitches, W.R., 1983. Pan-African structures, ophiolites and mélanges in the Eastern Desert of Egypt: a traverse at 26° N. Journal of Geological Society London 140, 75–95.

Roeder, P.L., 1994. Chromite from the Fiery rain of Chondrules to the Kilauea iki lava lake. Canadian Mineralogist 32, 729–746.

Shackleton, R.M., Ries, A.C., Graham, R.H., Fitches, W.R., 1980. Late Precambrian ophiolitic mélange in the Eastern Desert of Egypt. Nature 285, 472–474.

Shazly, A.G., Heikal, M.T., 1980. Geology and lithostratigraphy of Wadi El-Sodmein District, Eastern Desert, Egypt. Delta Journal of Science-Egypt 4, 268–292.

Wicks, F.J., Plant, A.G., 1979. Electron microprobe and X-ray microbeam studies of serpentine textures. Canadian Mineralogist 17, 785–830.

Yoder, H.S., 1967. Spilites and serpentinites. Carnegie Inst. Washington, Year Book 65, pp. 269–279.